
Article:
Zhang, Z., Provis, J.L. orcid.org/0000-0003-3372-8922, Zou, J. et al. (2 more authors) (2016) Toward an indexing approach to evaluate fly ashes for geopolymer manufacture. Cement and Concrete Research, 85. pp. 163-173. ISSN 0008-8846

https://doi.org/10.1016/j.cemconres.2016.04.007

Postprint of a paper published in *Cement and Concrete Research*, 85(2016):163-173. Version of record is available at http://dx.doi.org/10.1016/j.cemconres.2016.04.007

Toward an indexing approach to evaluate fly ashes for geopolymer manufacture

Zuhua Zhang [1, 2]*, John L. Provis [3], Jin Zou [4], Andrew Reid [5], Hao Wang [1]*

1. Centre for Future Materials, University of Southern Queensland, West Street, Toowoomba, Queensland 4350, Australia.

2. Fundamental Science on Nuclear Wastes and Environmental Safety Laboratory, Southwest University of Science and Technology, Mianyang 621010, China.

3. Department of Materials Science and Engineering, The University of Sheffield, Sheffield S1 3JD, United Kingdom.

4. School of Mechanical and Mining Engineering, and Centre for Microscopy and Microanalysis, The University of Queensland, St Lucia, Queensland 4072, Australia.

5. Haald Engineering Pty Ltd, Suite 5B, 19 Lang Parade, Milton QLD 4064, Australia.

*(*corresponding authors: Zuhua.Zhang@usq.edu.au; Hao.Wang@usq.edu.au)*

Abstract

Variations between fly ashes can lead to significant differences in the geopolymers derived from them, in both microstructural and mechanical properties. This study assesses the effect of physical, crystallographic and chemical characteristics of fly ash on geopolymerisation performance and the strength of the resulting binders. Physical and glass chemistry factors are combined to develop a comprehensive index to evaluate the suitability of fly ashes for the production of high-strength geopolymers. An equation for this index is proposed, developed using five typical low-calcium fly ashes and then validated against a further eight literature datasets, showing a good relationship between the ranking order of the calculated index and the compressive strengths of geopolymer pastes produced with comparable activator and paste

workability. This index can be used to screen the source materials, which is of significant value in moving alkali activated cements towards acceptance in practice.

Keywords: Alkali activated cement; Fly ash; X-Ray Diffraction; Compressive Strength

1. Introduction

With demand driven by environmental protection and waste utilisation, alkali-activated aluminosilicate materials, also known as geopolymers, have been developed rapidly in the last two decades and are increasingly regarded as promising green alternatives to Portland-based cements [1]. Accordingly, geopolymers based on alkali activation of fly ash have been extensively studied. Fly ash-based geopolymer technology is considered particularly attractive for commercialisation in areas of the world where this precursor is available in large volumes including Australia, China and the United States. Its lower activator requirement, compared to metakaolin, which is another type of widely used raw material, means that fly ash-based geopolymer can be produced at a low cost.

Some demonstration projects have been constructed using geopolymer concretes made from alkali activated fly ash blended with certain proportions of slag [2]. However, large-scale manufacture of fly ash-based geopolymer still progresses slowly and faces some technical and regulatory obstacles [3]. Among these, the inconsistent properties of fly ash (between sources, and from time to time from a single source) may be the most critical technical issue hindering large-scale deployment. Variations in the chemical compositions of coal sources, and the details of the combustion processes applied in different facilities worldwide, result in significant differences in terms of the chemical and physical characteristics of the resulting fly ashes. These variations lead to varying properties and performance levels in the geopolymers

produced, as has been demonstrated using fly ashes obtained from different sources worldwide [4-6]. This hinders the acceptance of geopolymer concrete by the civil engineering and construction industries, as the relationship between mix design parameters and performance is not as readily predictable as is the case for Portland cement-based systems, which necessitates extensive laboratory testing prior to the use of any particular geopolymer mix design, and means that ongoing quality control throughout a production run is essential. To solve this problem, it is necessary to construct effective assessment methods to determine the performance of fly ashes in geopolymer mixes and predict their likely strength development based on readily-assessed material parameters.

In previous studies [4-6], it has been found that key factors affecting the compressive strength development of fly ash-based geopolymers include particle size distribution, the content of glassy phases and the content of glass network modifying species (mainly alkali and alkali earth metals). The avoidance of excessive unburnt carbon content is also important [7], but the regulatory loss on ignition limits which are imposed on fly ashes sold for blending with cement and concrete are likely to be sufficient to ensure that this parameter is not problematic in their use in geopolymerisation. It may thus be expected that a fly ash with small particle size, high glass content and high network modifier content would yield high compressive strength of the derived geopolymer. However, a model built from a single parameter is not sufficient to correlate with the mechanical performance of the resulting geopolymer [5, 8]. For example, the Class C fly ash 'BY' used by Diaz et al. [5] showed the fastest setting (1.5 min) in alkali-activation among five ashes tested by those authors because of its high content of CaO (22.45%) and the finest particles, but resulted in the formation of a geopolymer with the second highest compressive strength; in comparison, the fly ash 'ML', which had the second-highest amount of CaO and the second-highest amount of glassy phases, exhibited the highest geopolymer strength.

More fundamental understanding is expected to come from detailed analysis of the content and chemistry of the glassy phases in fly ashes, but this is complicated by the heterogeneity of the glasses, within and between particles even in ash from a single source. By using quantitative X-ray diffractometry (XRD), electron microscopy and selective dissolution techniques, it is possible to determine the quantity and composition of the glassy phases in a fly ash [9-14]. The network modifier content and Si/Al ratio in the glassy fraction are considered to be two critical factors that play important roles in determining the dissolution of fly ash [15] in geopolymerisation, and these parameters have also been linked into a single descriptor through the introduction of 'optical basicity' as a proposed (but not yet widely used) measure of fly ash chemistry [16]. Fe is another important element present in many fly ashes and it brings more complexity for the understanding of geopolymerisation, as its role in the glass dissolution and gel formation processes is yet to be fully defined [17-19].

There is thus an evident need for a comprehensive index, considering not only chemical but also physical properties of fly ash, to be able to effectively evaluate the 'grade' of a fly ash in terms of its suitability for geopolymer manufacture, where predictable and consistent performance is critical in the absence of any performance-buffering effect from a manufactured Portland cement clinker component as is the case for blended cements. In this study, we demonstrate one such indexing concept, enabling effective evaluation of the suitability of fly ashes for the manufacturing of high strength geopolymers. Physical, chemical and crystallographic properties of five typical low-calcium Australian fly ashes are characterised and used to develop a reactivity index from theoretical grounds, and the effects of these parameters on geopolymer formation are examined. In combination with the understanding of glass chemistry which is available in the literature, a comprehensive index to correlate the characteristics of fly ash with the strength of geopolymer products is proposed for the first time,

and validated against a broader set of literature data for low-calcium fly ashes reacting to form geopolymers.

2. Experimental programme

2.1 Materials

Five Australian fly ashes, obtained from Gladstone, Millmerran, Callide, Eraring and Tarong power stations, were used in this study, and are denoted as A, B, C, D and E for brevity. Fly ashes from these power stations, except for Millmerran, have been studied previously in work including [4, 14, 18, 20], and relevant information can be obtained from those studies for comparison. An alkaline activating solution was formulated by blending a commercial sodium silicate solution (Na_2O=14.7% (mass), SiO_2=29.4%, D-Grade ™, PQ Australia) with 12 M NaOH solution to reach the desired modulus (molar ratio SiO_2:Na_2O) of 1.0 and concentration of 36.7 wt.% of (Na_2O + SiO_2). This activator was allowed to equilibrate to room temperature prior to use. Deionised water was used throughout all experiments.

2.2 Fly ash characterisation

The key parameters of the fly ashes include particle size distribution, specific surface area (SSA), particle density, particle packing density, bulk composition and mineralogical composition. Particle size distributions of the five samples were determined using a laser diffraction particle size analyser (PSA, Malvern Mastersizer 2000). SSA was determined from the PSA results assuming spherical particles (geometric surface area), and was also measured by the Brunauer-Emmett-Teller (BET) method using nitrogen sorption on a Micromeritics TriStar II 3020 instrument (accessible surface area). Particle density was determined by the

Archimedes method, using acetone and a volumetric flask. Particle packing density was simply determined as the ratio of weight to volume of each ash in a graduated container following 1 min of shaking by hand. Three replicate tests were conducted for each fly ash to obtain an average particle packing density. The mass loss which takes place upon heating was determined by thermogravimetric analysis (TGA) using a TA Q500 instrument under ambient air, heating at 10°C/min from room temperature to 800°C. The content of carbonaceous particles (which will include organics as well as carbonates) was defined as the mass loss at higher than 450°C, where the contribution to loss on ignition below this temperature is attributed to superficial hydration.

Bulk fly ash composition was determined using an ARL-9800 X-ray fluorescence (XRF) instrument (Thermo Scientific), including loss on ignition analysis at 1000°C in air. The mineralogical components, including crystalline and glassy phases, in each fly ash were identified by X-ray diffraction (XRD) and quantified by Rietveld refinement. The XRD data were collected using an ARL 9900 Series X-ray workstation (Thermo Scientific) with Co Kα radiation, operated at 40 kV and 40 mA, with a step size of 0.02° and count time 4 s/step from 8 to 80° 2θ. Each fly ash sample, without any classification or grinding, was mixed with 20% corundum (α–$Al_2O_3 \geq 99.99\%$, Aladdin), as an internal standard. The error of this quantitative XRD technique is assessed by comparing the quantities of each phases determined at three levels of internal standards (20%, 15% and 10%). The morphologies of fly ash samples and dried geopolymer samples, coated with gold, were analysed using a JEOL JCM-6000 scanning electron microscope (SEM) at high vacuum, with 15 kV accelerating voltage. To better understand the composition distribution (particularly for Fe and Ti) of glass and crystalline phases, selected fly ash samples were also etched with 1 M NaOH solution and analysed with energy dispersive spectroscopy (EDS).

2.3 Geopolymer synthesis and test procedure

Pastes were formulated initially at a target activator/ash ratio of 0.39 (Table 1). At this ratio the mixtures based on ashes A and C exhibited favourable workability; however, because of the varying particle properties of the ashes, pastes B, D and E required small amounts of additional water during mixing to achieve similar workability, as measured by using a minislump test. The addition of water has changed the concentrations of the dissolved activator components but not the modulus of the activator or the dose of alkalis with respect to the mass of fly ash (Table 1). The activator concentration is a parameter that can affect the geopolymerisation rate at early age, but will not necessarily change the total reaction extent, as indicated by the equivalence of the total heat released by systems with the same Na_2O content at differing water contents in calorimetric testing [21]. To supplement these tests and enable comparisons to be conducted also on the basis of constant activator chemistry, a second set of pastes were prepared by activation of fly ashes A, B and E with an activator mixed with water to match the diluted activator (activator plus water) used for ash D, at liquid/solid ratios yielding comparable workability for each ash (samples A_L, B_L and E_L, Table 1). There are thus two sets of samples available for direct comparison: samples A, B, C, D and E are formulated at constant activator (Na_2O+SiO_2) dose and modulus but with differing activator concentrations, while samples A_L, B_L, D and E_L are formulated at constant activator concentration but with different doses.

The paste specimens were cast in cylindrical moulds of ø52.5 mm × 105 mm, sealed and cured in an oven at 40°C for 1 day. After this time, they were taken out of the oven, allowed to cool, and aged at 25±2°C, still kept sealed. The hardened specimens were demoulded at 28 days and tested for compressive strength using a MTS universal mechanical testing machine at a loading-

head movement rate of 0.5 mm/min. To obtain parallel two end-faces, the top surface of each cylindrical specimen was sanded flat and the bottom face was capped with sulphur mortar.

3. Results and discussion

3.1 Physical properties

Fig.1 shows SEM images of the fly ashes, in which fly ashes A and C can be found to have more spherical particles while the other three fly ashes have much larger but irregular particles. Spherical shape is beneficial in the manufacture of geopolymers as it results in good workability at low liquid/solid ratios [22], and this is consistent with the fact that A and C are the two ashes from which geopolymers could be produced with no additional water required to achieve acceptable workability (Table 1). Fly ashes B and E contain many irregular particles, which may require a thicker liquid layer on the surface to overcome friction and enable particle sliding. In fly ashes A and B there are many very fine (<5 µm) spherical particles accumulated on the surfaces of the relatively large particles. These very fine particles can contribute high surface area and increase the initial dissolution rate of the fly ash.

Fig. 2 plots the particle size distributions of the five fly ashes as determined by laser diffraction. The ashes all have more than 75% (by volume) of particles smaller than 45 µm, a standard limit for fly ash used in cement as per Australian standard AS3582.1 [23]. The median particle size (D_{50}) of each of the fly ashes is given in Table 2. Fly ash A has the smallest particle size, with a D_{50} of 7.6 µm. Fly ashes B and D are in the middle with D_{50} values of about 20 µm, while fly ashes C and E are the largest, at about 30 µm. The geometric SSA of fly ash is calculated from the particle size distribution data using the assumption that the particles are spherical (Eq.1), and the results are listed in Table 2. Fly ash B has the highest geometric SSA due to its high volume of ultrafine particles below 1 µm (Fig. 2), followed by fly ash A, while fly ash E has

the lowest surface area. The geometric SSA values can also be compared to the values of accessible surface area, directly measured by the BET method. As expected, the geometric SSA values are lower than the BET SSA because of the ability of nitrogen sorption to probe internal as well as external surface area, in addition to the underestimation inherent to laser particle analysis where irregular particles are assumed to be perfectly spherical.

$$\text{Geometric SSA} = \frac{0.60/D[3,2]}{Particle\ density} \quad \text{(Eq.1)}$$

Besides the influence of particle shape, carbonaceous particles also affect the SSAs and liquid requirements of the ashes. Unburnt coal particles have much higher SSA, usually between 20-60 m^2/g [24], due to their internal porosity which is accessible to nitrogen in the BET method. For the purposes of this study, it is proposed that the geometric SSA calculated by particle size distribution is a more representative value to use in the evaluation of the effects of the particle size of fly ash on geopolymer properties, as it excludes the possible effect of carbonaceous particles.

In the geopolymer mixing process, the activator solution wets the fly ash particles, forming a layer of liquid on the surface, as illustrated in Fig. 3. The volume of this surface layer (denoted SLV) is directly related to the geometric SSA, if it is assumed that the thickness is uniform for all particles. The geometric SSA is thus an important property governing the activating liquid requirement of fly ash, and is also an important physical property affecting the dissolution of fly ash in geopolymerisation, thus influencing the compressive strength of the derived geopolymers [25]. Although it is likely that some of the very fine particles will differ significantly in reactivity from the bulk fly ash glasses (e.g. alkali sulfate particles), the description used here is a first-order approximation assuming broadly similar reactivity across all particles regardless of size. This is likely to be more realistic for some ashes than others,

and should be revisited in future extension of the model concept presented here, but is a necessary simplifying assumption at this point.

According to Table 2, fly ash B, with the highest geometric SSA, is expected to have the fastest dissolution and geopolymerisation. However, geopolymer A demonstrated the highest strengths under the two activating conditions (Table 1), suggesting that other factors must play key roles in determining the compressive strength. On this basis, we introduce an additional geometric parameter, the inter-particle volume (denoted IPV), as a physical characteristic of fly ash to be incorporated into the ash activity index calculation. As indicated in Fig. 3, when polydisperse particles are randomly packed, small particles fill in the empty spaces between large particles to increase the packing density [26]. However, there are still gaps between particles, forming the IPV. When a liquid activator is mixed with a dry fly ash powder, the SLV contributes to wetting the fly ash particles, while at the same time, additional liquid is required to fill the IPV, lubricating the system to provide necessary workability to the paste by enabling it to become a coherent fluid rather than a partially-cohesive granular system. This concept is somewhat similar to those concepts of filling water and layer water in cement systems [27]. The smaller the IPV, the less liquid is required to achieve this. From this point of view, the total liquid requirement for a geopolymer system is the sum of the SLV and IPV. More importantly, after geopolymerisation and hardening, some of the excess liquid will eventually evaporate once the sample is exposed to a relative humidity of less than 100% (including if self-desiccation takes place), leaving a certain volume of space which becomes pores the in hardened binder. Therefore, a smaller IPV can generate a more compact binder with a lower porosity, which usually means a higher strength [28].

For a given mass of fly ash, the IPV can be determined by subtracting the particle volume (mass/particle density) and the SLV from the total volume (mass/packing density), alternatively, by subtracting the SLV from the total liquid volume. The calculation of SLV

needs specific layer thicknesses for each fly ash, which means the shape factor of each fly ash particles can affect the real thickness in mixing. Given the relatively spherical shape of fly ash particles (shape factor close to 1), the thickness of the liquid layer is assumed to be uniform at 24.9 nm [27] and it is thus possible to estimate the values of SLV, and consequently the IPV. Fig. 4 shows the IPVs and geometric SLVs of fly ashes and the corresponding compressive strengths of the derived geopolymers. The evident correlations between the 28-day strength and other two physical characteristics suggest that strength is generally proportional to SSA, but decreases with increasing IPV, consistent with the suggestion that this parameter is linked to the porosity of the hardened paste.

It is also interesting to note that the trend in strength for the A_L, B_L, D and E_L samples (with constant activator composition) follows relatively closely the trend in the A, B, D and E samples (with constant activator dose). Sample B_L has a significantly lower strength than sample B despite its lower liquid/ash ratio and higher activator dose, which may be related to moulding/casting defects associated with the less favourable flow properties of this mix, while the higher activator dose in E_L compared to E was sufficient to yield a higher strength despite the higher overall liquid content of E_L. The main purpose of this comparison was to demonstrate that the trends in strength between ash sources are maintained regardless of the mix design basis of the geopolymer formulations, and thus that the ash activity index calculations can be applied as comparisons between ashes whether constant activator dose or constant activator composition are used in designing each mix.

3.2 Crystallographic characteristics

Table 3 lists the compositions of the five fly ashes, determined by XRF; all of the ashes are rich in Si and Al, and contain low concentrations of Ca and other components. All would be

classified as Class F according to ASTM C618 [29], or as siliceous according to EN 197-1 [30]. However, bulk composition is less effective as a direct link with the reactivity of fly ash, as highlighted in previous studies [13, 14, 17]. The crystalline phases, usually mullite, quartz and magnetite, in fly ash particles remain relatively inert throughout the early stages of alkaline dissolution and geopolymerisation; only the glassy phases are dissolved and participate in the reaction process during this time. From this point of view, the use of molar ratios based on bulk chemical compositions, which is used in much of the academic literature for geopolymer mix design, is actually giving very limited information in the case of fly ash geopolymerisation. The direct use of glassy phase compositions, rather than the overall ash composition, to formulate geopolymer binders is considered to give more appropriate descriptions of the gel chemistry, and this principle has recently been adopted in published studies [18, 20].

Table 4 shows the glass contents of the five fly ashes determined by Rietveld refinement of XRD data. These calculated glassy contents may be considered as an upper bound because they are based on a simple mass balance, assuming that all of the remaining components except for the crystalline phases detected by XRD are glassy. In reality, there may be some other minor crystalline phases, such as calcium silicates, anhydrite, gypsum and carbonates, which are present at concentrations or particle sizes below the detection limit of the diffractograms obtained here, and these are considered negligible in the calculations. It is also noted that the ferrite spinel phases are quantified here as being pure iron oxides, where substitution of other cations (particularly Mg^{2+}) into these phases is known to take place in both European and Australian fly ashes [31, 32], and will alter the Bragg peak intensities compared to the pure compounds.

From the literature, it has been reported that a fly ash from the same source as ash A contains 70-80 wt.% amorphous phases [33], and that fly ashes from the same sources as C and E contained 76 and 68 wt.% glass, respectively [34]; it has also been reported in a separate study

that fly ashes from sources D and E contain 62.7 and 50.8 wt.% amorphous content, respectively [18]. The current quantified results are broadly consistent with those reported values.

The quantification of crystalline and glassy phases in each of the fly ashes shows that fly ash E has the lowest amount of glassy phases. If it is assumed that glassy phases are the reactive components in geopolymerisation, fly ash E will be expected to generate a binder with lower gel volume and thus potentially a lower strength. However, the amounts of glassy phases in the other four fly ashes are not significantly different compared to the variation between their strengths. In fact, fly ash will only achieve a certain reaction extent during geopolymerisation, e.g. in the range 15 to 35% after 48 h curing at 65°C and 7 days ageing at 25°C [35, 36], although this may be increased to up to 60% by extending high temperature curing to 7 days at 85°C [37]. The reaction extents of fly ashes in this study are also low, and a large fraction of particles remained with only partial dissolution of the glassy parts (Fig.5). This implies that the quantity of glassy phases is likely to be a secondary factor which influences but does not directly control geopolymerisation and consequent strength development, as long as the glass fraction of the ash is sufficient to enable the reaction to actually take place to a satisfactory extent.

3.3 Chemical characteristics of glassy phases

The overall glass phase compositions in each of the fly ashes studied can be calculated by subtracting the crystalline phases from the bulk compositions, and are shown in Table 5. However, it must be noted that the glassy phases in fly ash are also heterogeneous, usually with different localised compositions, depending on the original minerals present in the pulverised coal, and also on the phase segregation and liquid-liquid immiscibility which is observed during cooling of the ash particles in the chimney of the boiler [9, 34, 38]. Fig. 6 shows the

SEM-EDS analysis of selected fly ash particles after NaOH dissolution. It can be seen that Si and Al are the dominant elements in each of the glasses, along with Fe in fly ash A.

In aluminosilicate glasses, Si is almost exclusively present as a network former in four-fold coordination, i.e. $^{[4]}Si^{4+}$. The role of Al is complex because of its varying coordination states, i.e. $^{[3]}Al^{3+}$, $^{[4]}Al^{3+}$, $^{[5]}Al^{3+}$ and $^{[6]}Al^{3+}$. Guillot and Sator [39] studied natural silicate melts with 35-75 wt.% SiO_2 and 5-15 wt.% Al_2O_3 (the rest includes CaO, FeO and TiO_2, the composition is close to that of fly ash), and showed that Al mainly acts as a network former, with 71–75% of $^{[4]}Al$, but also as a modifier with 12–22% of $^{[5]}Al$. In the glassy phases of fly ash, the relative concentrations of network forming and modifying Al will change according to the local composition, spinodal decomposition processes during cooling, the diffusion of alkali and alkali earth metals, and the thermal history. For example, in the CaO(MgO)-Al_2O_3-SiO_2 glasses, the network forming $^{[4]}Al$ decreases from 100% to 60% as the MO/(MO+Al_2O_3) molar ratio decreases from 0.5 to 0 [40]. This is because there are not sufficient charge balancing cations and a proportion of the Al may thus be required in a network-modifying role.

The thermal history is also important to the role of Al. In the calcium aluminosilicate glasses, the concentration of $^{[5]}Al$ slightly increases from 5% to 10% as the heating temperature increases from 800 to 1000°C (also varying with Ca content) because of the thermal activation of $^{[4]}Al$ into $^{[5]}Al$ [41]. Fly ash glasses usually form at higher temperatures (1400-1700°C), which means there is possibility of a certain amounts of $^{[5]}Al$ existing. Solid-state magic-angle spinning nuclear magnetic resonance (MAS NMR) analysis showed that fly ashes contain a small amount of $^{[6]}Al$ and a trace amount of $^{[5]}Al$ (could be <5% according to the spectra shape), in addition to the majority $^{[4]}Al$ [42]. The $^{[6]}Al$ represents the octahedral Al in crystalline phases, such as mullite, or in glasses with local structures resembling these phases, while $^{[5]}Al$ represents the network modifying Al in the glass. However, as indicated in the discussion above, the relative content of $^{[5]}Al$ is usually much lower than $^{[4]}Al$, and in this study, the Al is broadly

assumed to be a network former to simplify its incorporation into index calculations, in agreement with the NMR analysis of a typical Class F fly ash [43].

Nevertheless, the presence of more Al in the glassy phases usually means a higher reactivity of the fly ash because of the weaker bonding of Al-O compared to Si-O [44]. The availability of Al is critical to the properties of geopolymers [45, 46]; fly ash with large amounts of reactive Al (low Si/Al ratio) can generate a high amount of geopolymer reaction products, although its dissolution rate may be low [47]. Brindle & McCarthy [10] found that for a large suite of European coal ashes, high Al content and high alkali content in the glassy phase were closely correlated, but this does not appear to be the case for the Australian ashes investigated here.

Fly ashes B and C have high Al contents, which could be one of the reasons for the relatively higher strengths of the geopolymers derived from these ashes. Si and Al act as the framework formers of geopolymer gels, and the ratio between the availabilities of these components, from both the solid precursor and the activator, influences the mechanical properties of geopolymers [20, 45, 46, 48]. However, Němeček et al. [49] reported that there was no evident correlation between chemical composition of geopolymeric gels and the elastic modulus, indicating that Si/Al ratio of geopolymeric gels could be a secondary factor that governing the mechanical properties of a geopolymer. Other factors, including activator and solid precursor chemistry, and dissolution rate effects and the porosity of hardened gels, must also be taken into consideration.

Among the five fly ashes the concentrations of alkali metals (mainly Na and K in fly ash, denoted M) and alkali earth metals (mainly Ca and Mg, denoted Me) vary significantly. In aluminosilicate glasses, these elements can act as network modifiers, forming non-bridging oxygen sites [50] thus potentially reducing the degree of polymerisation of the aluminosilicate glasses if present at high enough concentrations. Glasses with charge-balanced compositions

of $(M_2O+MeO)/Al_2O_3 = 1$ still show the depolymerisation influence of alkali and alkali earth metals [51], and a higher concentration of such elements usually means higher reactivity of the glassy phase of fly ash, either in Portland cement system [9] or in alkali-activated system [5]. Such a trend can be found in the five ashes investigated here.

In addition to Si, Al and the network modifiers, Fe and Ti are also present at relatively high concentrations in the glassy phases of the five fly ashes (Table 5). The concentrations of Fe and Ti listed in Table 5 as being present in the glass phases which should be considered to be upper bounds, as the quantification is based on the assumption that the crystalline phases used in the Rietveld refinement are pure. In fact, mullite grains present in fly ash usually include substitution of Fe and Ti for several percent of the Al [31]. However, considering the low substitution ratios, this simplification appears appropriate, and is consistent with other studies [18, 32].

In a fly ash, the Fe expressed as Fe_2O_3 in the XRF analysis of the glassy part is actually a mix of two oxidation states, i.e. divalent Fe (Fe^{2+}) and trivalent Fe (Fe^{3+}). The local environments of Fe^{2+} and Fe^{3+} are complex in silicate glasses, which commonly include $^{[4]}Fe^{2+}$, $^{[5]}Fe^{2+}$, $^{[4]}Fe^{3+}$, and $^{[5]}Fe^{3+}$. The real states of Fe and their relative concentrations depend on the thermal history of the coal combustion process, and the concentration of Fe and other elements in each particle. In the $FeO-Fe_2O_3-SiO_2$ glass system, with a low concentration of Fe (Fe:Si < 1:5) and at 2000 K, Si and Fe tend to form cristobalite and a liquid phase which contains fourfold and fivefold coordinated Fe, while at 1730 K, Si and Fe tend to form separate phases, such as magnetite and tridymite, or hematite and tridymite at lower temperatures [52]. This means that if Fe atoms tend to segregate into locally Fe-rich or crystalline phases and are in a 6-coordinated environment, for example when the fly ash is formed at a relatively low temperature or is cooled less rapidly, Fe has limited capability to substitute for Si in the glass network. However, as evidenced by the SEM-EDS analysis [53] and the SEM-EDS analysis in this study (Fig. 6),

Fe can be distributed in the amorphous aluminosilicate glass throughout the fly ash particles. This is either because of the high combustion temperatures or the flexibility introduced by M and Me substitution, or both. As a result, fourfold coordinated Fe^{2+}/Fe^{3+} and fivefold coordinated Fe^{2+}/Fe^{3+} should both be present in fly ash glass.

The distribution of Fe is heterogeneous in fly ash glass, but for the sake of comparison between ashes based on bulk properties here, only the overall concentrations are considered. Even if it is assumed that the glassy part of fly ash is homogeneous, the role of Fe in aluminosilicate glass chemistry is still very complex. The glassy phase of fly ash contains certain amounts of Al, as well as alkali and alkali earth cations. It is known that in aluminosilicate glass, Fe^{2+} cations are mainly in the 5-coordinated state, acting as network modifiers; Fe^{3+} can be 5-coordinated to act as a network modifier as well, but is also partially in the 4-coordinated state and acting as a network former, analogous to the role of Al^{3+} [54]. The relative concentrations of Fe acting as network modifiers and formers will depends on a range of factors, such as the Al/Si ratio, the concentrations of alkalis and alkali metals, the availability of excess oxygen during coal combustion and ash cooling, and others. It is reported that in silicate glass melts, as the ratio of $(Na_2O+K_2O)/Al_2O_3$ increases from 1.04 to 1.81, the Fe^{3+} fraction (among total Fe^{2+} + Fe^{3+}) increases, and its role as network former increases in general [55]. The low $(Me_2O+MO)/Al_2O_3$ ratio in the ashes studied here is expected to yield a high concentration of Fe^{2+} in the fly ashes according to the general trend proposed in [55]. Nevertheless, the high concentrations of Fe in glass phases of fly ashes A and C are expected to yield a high fraction of fivefold coordinated Fe^{2+} and Fe^{3+}, which decreases the polymerisation degree of glass and thus increases the reactivity of fly ash.

Titanium also plays a complex role in silicate glasses. In alkali metal bearing glasses, Ti^{4+} is present in a 4-coordinated state at low concentration, but is predominantly in 5-coordinated at

higher concentration, depending on the glass composition including the nature and types of alkali metals present [56]. In addition to alkali and alkali earth metals, the glassy phase of fly ash also involves Al and some Fe, making the structural role of Ti yet more complex. However, as the TiO_2 content is relatively low in fly ash (usually <2 wt.%), Ti^{4+} is expected to act as a 4-coordinated network former, particularly given the heterogeneous distribution of Ti and the trend of alkali and alkali earth metal cations, and some of the Fe, acting as charge compensators for Al and Fe tetrahedra.

3.4 The development of a reactivity index

For the commercial scale application of fly ash geopolymer technology, the industry desires a set of standard methods to assess the suitability of locally available fly ashes. As discussed above, the critical parameters which have been identified in this study include the SSA and IPV of the particles, and the chemical properties of the glass. The relative weightings of these parameters in terms of their influence on the final strength of geopolymers are different, and require analysis by more systematic approaches. The eventual goal is to develop a single and comprehensive index to evaluate the suitability of fly ashes for manufacturing high strength geopolymer. From this concept, a general format for such an index can be sketched as:

$$I = f(\text{SSA}) \cdot f(\text{IPV}) \cdot f(\sum a_i X_i) \qquad \text{(Eq.2)}$$

in which f(SSA) and f(IPV) are the functions of specific surface area and inter-particle volume, respectively; and $f(\sum a_i X_i)$ refers to the effect of glass chemistry, where a_i is the coefficient of each elemental parameter X_i in the glass fraction. These parameters include the concentrations of glass network formers (Si, Al, Fe, Ti) and network modifiers (Na, K, Ca, Mg, Fe), as well as parameters such as sulfate content and loss on ignition which are not considered explicitly

in this study but may become significant for some ash sources. The relationships between each factor and the strength of the resulting geopolymer can be assessed separately to determine the a_i values, although this would require substantial and systematic research on each factor with the full control of the other factors, and this is not feasible in a laboratory or plant trial setting.

Although the detailed format of this equation is not able to be given at the current point in time, a preliminary equation is proposed to simply link all of the factors examined in this study, for ashes which are relatively low in calcium and thus rely on glasses rather than crystalline calcium-containing phases to provide their reactivity:

$$I = \frac{SSA}{IPV} \times \frac{Total\ charge\ of\ network\ modifers\ (c_{NM})}{Molar\ number\ of\ network\ fomers\ (n_{NF})} \quad \text{(Eq.3)}$$

This simplification is based on the following considerations and assumptions: (1) a roughly linear relationship between the SSA and compressive strength of geopolymers is found by correlating the data of Kumar and Kumar [25]; (2) compressive strength is assumed to be inversely related to the IPV; and (3) the dissolution of glassy phases is assumed to be incomplete (this is in agreement with the real situation, Fig. 5) with an extent proportional to the molar concentrations of network modifiers due to their depolymerisation influence, which is further assumed to depend on the total charges of each modifier.

To calculate the value of this index, it is necessary to determine the concentrations of 5-coodinated Fe ions, i.e. $^{[5]}Fe^{2+}$ and $^{[5]}Fe^{3+}$, which depend on a number of parameters of the glass, such as the Si/Al ratio and the concentrations of M and Me [54, 57]. The concentrations of these elements in glasses can be quantified using neutron diffraction and Empirical Potential Structure Refinement (EPSR) modelling methods [58], although this has not yet been undertaken for fly ashes. In this study, the fractions of $^{[5]}Fe^{3+}$ and $^{[5]}Fe^{2+}$ are approximated by

using the linear relationships between Fe^{3+}, total Fe, and the total charges on Ca^{2+}, Mg^{2+}, Na^{+} and K^{+} obtained by fitting the results of Weigel et al. [58], with results as shown in Table 6.

Using the combination of the determined SSAs (Table 1), the calculated IPVs (Fig. 4) and the total concentrations of network modifiers and formers in glassy phases, the index for the five fly ashes can be calculated, and the results are given in Table 6. The index of fly ash A is the highest, 1.29, followed by fly ash B, 0.70. A general trend that the index decreases from fly ash A to E matches the ranking order of the strength of the derived geopolymers. However, the index of fly ash E is 0.05, which is markedly lower than the others, whereas the strength of the geopolymer is only slightly lower than for ash D. It seems likely that the relative contributions of SSA, IPV and network modifiers are not simply linearly related, and this requires more study to further refine the parameters of the proposed index equation. In particular, the relative influences of different cations on the dissolution and geopolymerisation of the glassy part of the ash is expected to differ from simple charge proportionality. This aspect is being investigated and will be reported in the future.

3.5 Application of the reactivity index

Applying the developed reactivity index to evaluate the fly ashes in selected literature studies of geopolymer manufacture [8, 20, 42] can show the powerful capability of this approach. In Table 7 eight fly ashes were re-examined in terms of their SSA, IPV and glass chemistry. The Gladstone, Eraring and Tarong fly ashes were sourced from the same power stations as the three used in this study but all had different chemical and physical properties due to having been sampled at different times. According to the compositions of the glassy phases and the particle geometric parameters it is possible to calculate the reactivity index *I* of each of the fly ashes. The order of *I* values matches perfectly with the ranking of compressive strengths of the

derived geopolymers in each of the manufacturing conditions. From reference [18], it is known that the compressive strengths of geopolymers changed significantly as the Si/Al ratio was manipulated using dissolved silica fume and sodium aluminate solutions. However, at a given ratio, the order of the compressive strengths always follows the order of the reactivity index. However, it must be noted that the sets of compressive strength data obtained from different studies cannot be compared directly although the reactivity index of each of the eight fly ashes is basically dependent on its nature. This is because that the activator and curing conditions varied in each study examined. To develop an approach to predict the strength development, the match of activator based on the feedstock characteristics and the optimisation of curing must be considered to achieve a high reaction extent (complete reaction of glassy phases seems unachievable at this stage). The index concept proposed in this study can only approach the problem from the feedstock perspective, and must be coupled with developments in other areas to provide a holistic prediction of geopolymer characteristics.

The result shown in Table 7 suggests that in geopolymer manufacture we can firstly screen the source of fly ashes by reactivity index and then design the composition accordingly. The index concept developed and presented here appears to have significant scope for predictive power in characterising the reactivity of different fly ashes in geopolymer synthesis, in terms of easily-measured parameters: particle size distribution and bulk glass chemistry. Although it is clear that further refinement of the index formulation is needed, and validation using a broader range of ash sources and activator compositions will be desirable in this regard, these results present important steps towards the ability to screen and control the performance of fly ashes for industrial-scale geopolymer synthesis.

4. Conclusions

The development of commercial scale fly ash-based geopolymer cement is still at a very early stage. To enable this new binder material to be fully adopted by industry, it is essential to more fully understand the heterogeneous nature of fly ash, and thus the influences of various physical, chemical and crystallographic factors on geopolymer formation and its properties. Five typical Australian fly ashes were the primary materials selected for development of a reactivity index in this study. In particular, their specific surface areas, inter-particle volumes and glassy components were shown to have significant impacts on the strength of the hardened geopolymers prepared by combining each ash with a sodium metasilicate activating solution. Based on these results and the data available in the literature, it was found that the concentrations of alkali and alkali earth metals, and Fe in reactive coordination environments, determine the reactivity of fly ash to a significant extent. In order to effectively evaluate the suitability of fly ashes for the manufacture of geopolymer binders, this study proposes a concept for combining these parameters into a single index. A preliminary form of this index has been developed, and is effective in ranking the strengths of the geopolymers derived from the five ashes studied, as well as the strengths of a further set of eight geopolymer mixes obtained from previously published literature. However, to further refine the index equation, more efforts are necessary to specify the relative contribution of each parameter. It is reasonable to believe that such a comprehensive index can prove to be a powerful tool in evaluating and grading the suitability of fly ashes for geopolymer formulation.

Acknowledgements

This study was sponsored by the Australian Research Council (LP130101016), and partially by a program funded by Fundamental Science on Nuclear Wastes and Environmental Safety Laboratory of SWUST (14zxnk01).

References

[1] C. Shi, A. Fernández-Jiménez, A. Palomo. New cements for the 21st century: the pursuit of an alternative to Portland cement. Cem. Concr. Res. 41 (2011) 750–763.

[2] J.L. Provis, S.A. Bernal, Geopolymers and related alkali-activated materials. Annu. Rev. Mater. Res. 44, (2014) 299–327.

[3] J.S.J van Deventer, J.L. Provis, P. Duxson. Technical and commercial progress in the adoption of geopolymer cement. Miner Eng 29 (2012) 89–104.

[4] J.G.S. van Jaarsveld, J.S.J. van Deventer, G.C. Lukey. The characterisation of source materials in fly ash-based geopolymers. Mater Lett 57(7) (2003) 1272–1280.

[5] E.I. Diaz, E.N. Allouche, S. Eklund, Factors affecting the suitability of fly ash as source material for geopolymers. Fuel 89 (2010) 992–996.

[6] S. Kumar, R. Kumar, T.C. Alex, A. Bandopadhyay, S.P. Mehotra. Influence of reactivity of fly ash on geopolymerisation. Adv Appl Ceram 106 (2007) 120–127.

[7] A. van Riessen, N. Chen-Tan. Beneficiation of Collie fly ash for synthesis of geopolymer: Part 1 – Beneficiation. Fuel 106 (2013) 569–575.

[8] Z. Zhang, H. Wang, J.L. Provis. Quantitative study of the reactivity of fly ash in geopolymerization by FTIR. J. Sust. Cem.-Based Mater. 1 (2012) 154–166.

[9] P.T. Durdziński, C. F. Dunant, M. Ben Haha, K.L. Scrivener. A new quantification method based on SEM-EDS to assess fly ash composition and study the reaction of its individual components in hydrating cement paste. Cem Concr Res 73 (2015) 111–122.

[10] J.H. Brindle, M.J. McCarthy. Chemical constraints on fly ash glass compositions. Energy & Fuels, 20(6) (2006) 2580–2585.

[11] J.C. Qian, E.E. Lachowski, F.P. Glasser. Microstructure and chemical variation in class F fly ash glass. In: Fly Ash and Coal Conversion By-Products: Characterization, Utilization, and Disposal IV, Warrendale, PA, 1988, Materials Research Society, 45–54.

[12] S.V. Vassilev, R. Menendez, D. Alvarez, M. Diaz-Somoano, M.R. Martinez-Tarazona. Phase-mineral and chemical composition of coal fly ashes as a basis for their multicomponent utilization. 1. Characterization of feed coals and fly ashes. Fuel 82 (2003) 1793–1811.

[13] A. Fernández-Jiménez, A.G. de la Torre, A. Palomo, G. López-Olmo, M.M. Alonso, M.A.G. Aranda. Quantitative determination of phases in the alkali activation of fly ash. Part I. Potential ash reactivity. Fuel 85 (2006) 625–634.

[14] R.P. Williams, A. van Riessen. Determination of the reactive component of fly ashes for geopolymer production using XRF and XRD. Fuel 89 (2010) 3683–3692.

[15] P. Duxson, J.L. Provis. Designing precursors for geopolymer cements. J Am Ceram Soc 91(12) (2008) 3864–3869.

[16] E.M. Gartner, D.E. Macphee. A physico-chemical basis for novel cementitious binders. Cem Concr Res 41 (2011) 736–749.

[17] N.W. Chen-Tan, A. van Riessen, C.V. Ly, D.C. Southam. Determining the reactivity of a fly ash for production of geopolymer. J Am Ceram Soc 92 (4) (2009) 881–887.

[18] W.D.A. Rickard, R. Williams, J. Temuujin, A. van Riessen. Assessing the suitability of three Australian fly ashes as an aluminosilicate source for geopolymers in high temperature applications. Mater Sci Eng A 528 (2001) 3390–3397.

[19] R.R. Lloyd, J.L. Provis, J.S.J. van Deventer. Microscopy and microanalysis of inorganic polymer cements. 2: The gel binder. J Mater Sci 44(2) (2009) 620-631.

[20] C. Tennakoon, P. De Silva, K. Sagoe-Crentsil, J. G. Sanjayan, Influence and role of feedstock Si and Al content in geopolymer synthesis. J Sust Cem-Based Mater 4(2) (2014) 129-139.

[21] X. Yao, Z. Zhang, H. Zhu, Y. Chen. Geopolymerization process of alkali–metakaolinite characterized by isothermal calorimetry. Thermochim Acta (493) (2009) 49–54.

[22] J.L. Provis, P. Duxson, J.S.J. van Deventer. The role of particle technology in developing sustainable construction materials. Adv Powder Technol 21 (2010) 2–7.

[23] AS3582.1: Supplementary cementitious materials for use with Portland and blended cement – fly ash. Standards Australia. 1998, Australia.

[24] J.Y. Hwang, X. Sun, Z. Li. Residual carbon in fly ash for mercury adsorption: I. Separation and characterization of unburned carbon. J Miner Mater Charact Eng 1 (2002) 39–60.

[25] S. Kumar, R. Kumar. Mechanical activation of fly ash: Effect on reaction, structure and properties of resulting geopolymer. Ceram Int 37 (2011) 533–541.

[26] E. Santiso, E.A. Müller. Dense packing of binary and polydisperse hard spheres. Molec Phys 100(15) (2002) 2461–2469

[27] M. Hunger. An Integral Design Concept for Ecological Self-Compacting Concrete. Ph.D. Thesis, Eindhoven University of Technology, 2010.

[28] D.M. Roy. New strong cement materials: Chemically bonded ceramics. Science, 253 (1987) 651–658.

[29] ASTM C618 – 12: Standard Specification for Coal Fly Ash and Raw or Calcined Natural Pozzolan for Use in Concrete. ASTM International. 2012: West Conshohocken, PA.

[30] EN 197-1:2011: European Committee for Standardization (CEN), Cement - Part 1: Composition, Specifications and Conformity Criteria for Common Cements. 2011: Brussels, Belgium.

[31] S. Gomes, M. François, M. Abdelmoula, P. Refait, C. Pellissier, O. Evrard. Characterization of magnetite in silico-aluminous fly ash by SEM, TEM, XRD, magnetic susceptibility, and Mössbauer spectroscopy. Cem Concr Res 29 (1999) 1705–1711.

[32] C.R. Ward, D. French. Determination of glass content and estimation of glass composition in fly ash using quantitative X-ray diffractometry. Fuel 85 (2006) 2268–2277.

[33] W.K.W. Lee, J.S.J. van Deventer. Use of infrared spectroscopy to study geopolymerization of heterogeneous amorphous aluminosilicates. Langmuir 19(21) (2003) 8726–8734.

[34] L. Keyte. What's wrong with Tarong? The importance of coal fly ash glass chemistry in inorganic polymer synthesis. PhD thesis. The University of Melbourne, 2008.

[35] U. Rattanasak, K. Pankhet, P. Chindaprasirt. Effect of chemical admixtures on properties of high-calcium fly ash geopolymer. Int J Miner Metal Mater 18(3) (2011) 364–369.

[36] P. Chindaprasirt, U. Rattanasak, C. Jaturapitakkul. Utilization of fly ash blends from pulverized coal and fluidized bed combustions in geopolymeric materials. Cem Concr Compos 33(1) (2011) 55–60.

[37] A. Fernández-Jiménez, A.G. de la Torre, A. Palomo, G. López-Olmo, M.M. Alonso, M.A.G. Aranda. Quantitative determination of phases in the alkaline activation of fly ash. Part II: Degree of reaction. Fuel 85 (2006) 1960–1969.

[38] K.L. Aughenbaugh, R.T. Chancey, P. Stutzman, M.C. Juenger, D.W. Fowler. An examination of the reactivity of fly ash in cementitious pore solutions. Mater Struct 46(5) (2013) 869–880.

[39] B. Guillot, N. Sator, A computer simulation study of natural silicate melts. Part I: Low pressure properties. Geochim Cosmochim Acta 71 (2007) 1249–1265.

[40] M.J. Toplis, D.B. Dingwell. Shear viscosities of CaO-Al_2O_3-SiO_2 and MgO-Al_2O_3-SiO_2 liquids: Implications for the structural role of aluminium and the degree of polymerisation of synthetic and natural aluminosilicate melts. Geochim Cosmochim Acta 68(24) (2004) 5169–5188.

[41] J.F. Stebbins, E.V. Dubinsky, K. Kanehashi, K.E. Kelsey. Temperature effects on non-bridging oxygen and aluminum coordination number in calcium aluminosilicate glasses and melts. Geochim Cosmochim Acta 72 (2008) 910–925.

[42] J.E. Oh, Y. Jun, Y. Jeong. Characterization of geopolymers from compositionally and physically different Class F fly ashes. Cem Concr Compos 50 (2014) 16–26.

[43] A. Palomo, S. Alonso, A. Fernandez-Jimenez. Alkaline activation of fly ash: NMR study of the reaction products. J Am. Ceram. Soc 87(6) (2004) 1141–1145.

[44] J.P. Hamilton, S.L. Brantley, C.G. Pantano, L.J. Criscenti, J.D. Kubicki. Dissolution of nepheline, jadeite and albite glasses: Toward better models for aluminosilicate dissolution. Geochim Cosmochim Acta 65(21) (2001) 3683–3702.

[45] A. Hajimohammadi, J.L. Provis, J.S.J. van Deventer. Effect of alumina release rate on the mechanism of geopolymer gel formation. Chem Mater 22 (2010) 5199–5208.

[46] A. Hajimohammadi, J.L. Provis, J.S.J. van Deventer. The effect of silica availability on the mechanism of geopolymerisation. Cem Concr Res 41 (2011) 210–216.

[47] S.L. Valcke, A.J. Sarabèr, P. Pipilikaki, H.R. Fischer, H.W. Nugteren. Screening coal combustion fly ashes for application in geopolymers. Fuel 106 (2013) 490–497.

[48] P. Duxson, J.L. Provis, G.C. Lukey, S.W. Mallicoat, W.M. Kriven, J.S.J. van Deventer. Understanding the relationship between geopolymer composition, microstructure and mechanical properties. Colloids Surf A 269 (2005) 47–58.

[49] J. Němeček, V. Šmilauer, L. Kopecký, Nanoindentation characteristics of alkali-activated aluminosilicate materials. Cem Concr Compos 33 (2011) 163–170.

[50] J. Stebbins, Z. Xu. NMR evidence for excess non-bridging oxygen in an aluminosilicate glass. Nature 390 (1997) 60-62.

[51] R.G. Kuryaeva. Degree of polymerization of aluminosilicate glasses and melts. Glass Phys Chem 30(2) (2004) 157–166.

[52] S. Ehrman, S. Friedlander, M. Zachariash. Phase segregation in binary SiO_2/TiO_2 and SiO_2 /Fe_2O_3 nanoparticle aerosols formed in a premixed flame. J Mater Res 14(12) (1999) 4551–4561.

[53] B.G. Kutchko, A.G. Kim. Fly ash characterization by SEM–EDS. Fuel 85 (2006) 2537–2544.

[54] L. Cormier, G. Calas, G. Cuello. Structural study of Ca-Mg and K-Mg mixing in silicate glasses by neutron diffraction. J Non-Cryst Solids 356 (2010) 2327–2331.

[55] G. Giuli, R. Alonso-Mori, M.R. Cicconi, E. Paris, P. Glatzel, S.G. Eeckhout, B. Scaillet. Effect of alkalis on the Fe oxidation state and local environment in peralkaline rhyolitic glasses. Am Mineral 97 (2012) 468–475.

[56] G. Henderson, M.E. Fleet. The structure of titanium silicate glasses investigated by Si K–edge X–ray absorption spectroscopy. J Non-Cryst Solids 211 (1997) 214–221.

[57] B.O. Mysen, D. Virgo, C.M. Scarfe, D.J. Cronin. Viscosity and structure of iron- and aluminum-bearing calcium silicate melts at 1 atm. Am. Mineral 70 (1985) 487–495.

[58] C. Weigel, L. Cormier, G. Calas, L. Galoisy, D.T. Bowron. Intermediate-range order in the silicate network glasses $NaFe_xAl_{1-x}Si_2O_6$ (x=0, 0.5, 0.8, 1): A neutron diffraction and empirical potential structure refinement modeling investigation. Phys Rev B 78 (2008) 064202–064212.

Postprint of a paper published in *Cement and Concrete Research*, 85(2016):163-173. Version of record is available at http://dx.doi.org/10.1016/j.cemconres.2016.04.007

Table 1. Compositions of geopolymer mixes and the calculated concentrations of Si and Na^+ of the activating solution based on the mass and ratio of 12 M NaOH solution, liquid sodium silicate and additional water. The 28-day compressive strengths are reported as the mean and standard deviation of 4 to 5 replicate tests.

Mix	Fly ash / g	Activator / g	H_2O / g	Liquid/ash / g / g	[Si]/ mol/L	[Na^+]/ mol/L	Compressive strength (28 d)
A	1000	390	0	0.39	4.3	8.8	52.8 ± 1.6
B	1000	390	160	0.55	3.1	6.6	43.7 ± 0.7
C	1000	390	0	0.39	4.3	8.8	35.1 ± 1.5
D	1000	390	100	0.49	3.4	7.0	16.5 ± 1.0
E	1000	390	230	0.62	2.7	5.5	12.8 ± 1.2
A_L	1000	280	70	0.35	3.4	7.0	32.5 ± 1.8
B_L	1000	360	90	0.45	3.4	7.0	24.8 ± 1.5
E_L	1000	480	120	0.60	3.4	7.0	14.5 ± 2.0

Table 2. Physical characteristics of fly ashes.

Fly ash	D_{50}, µm	Geometric SSA by PSA, m^2/g	Accessible SSA by BET, m^2/g	Carbonaceous, mass%	Particle density, g/cm^3	Packing density, g/cm^3
A	7.63	0.88	1.94	0.61	2.33	1.44
B	18.00	1.21	2.53	0.47	1.96	1.16
C	31.86	0.45	1.16	0.86	2.09	1.38
D	21.16	0.50	1.07	0.90	2.02	1.28
E	28.24	0.36	0.80	0.71	1.79	0.94

Table 3. Chemical compositions (wt.%) of fly ash as measured by XRF. LOI is loss on ignition at 1000°C; this is recorded for some ashes as being lower than the carbonaceous content measured by TGA due to the mass gain associated with oxidation of Fe^{2+} compounds between 850-1000°C.

Ash	SiO_2	Al_2O_3	CaO	MgO	K_2O	Na_2O	Fe_2O_3	P_2O_5	SO_3	TiO_2	LOI
A	47.5	27.3	4.25	1.48	0.54	0.74	14.3	0.91	0.29	1.47	0.53
B	53.3	32.5	6.90	0.90	0.59	0.27	3.10	0.10	0.30	1.60	0.50
C	54.4	32.1	1.06	0.75	0.22	0.14	7.49	0.09	0.04	2.14	0.85
D	67.3	22.5	1.00	0.53	2.11	0.50	3.74	0.09	0.07	0.90	0.90
E	71.2	24.7	0.08	0.12	0.53	0.01	1.16	0.04	0.02	1.42	0.43

Postprint of a paper published in *Cement and Concrete Research*, 85(2016):163-173. Version of record is available at http://dx.doi.org/10.1016/j.cemconres.2016.04.007

Table 4. The mineral compositions (mass %) of fly ashes as determined by Rietveld quantitative XRD method with 20 wt.% corundum as internal reference material.

Components (ICSD no.)	A	B	C	D	E
Glassy phase	74.2	81.7	75.8	78.4	62.8
Crystalline phases					
Mullite: $Al_{4.75}Si_{1.25}O_{9.63}$ (66448)	18.7			15.7	24.1
Mullite: $Al_{1.83}Si_{1.08}O_{4.85}$ (43289)		13.6	15.3		
Quartz: SiO_2 (89280)	3.1	2.6	6.5	5.0	13.1
Magnetite: Fe_3O_4 (43001)	2.5	1.3	2.4	0.9	
Hematite: Fe_2O_3 (15840)	1.5	0.8			
W_{RP}, %	*3.0*	*6.0*	*3.9*	*3.3*	*5.0*

Table 5. Chemical compositions in the glassy phases of fly ashes as calculated from the bulk compositions and mineral compositions. 'Others' includes P_2O_5, SO_3, trace components and LOI, mass%.

Fly ash	SiO_2	Al_2O_3	CaO	MgO	K_2O	Na_2O	Fe_2O_3	TiO_2	Others
A	54.0	17.5	5.7	2.0	0.7	0.9	13.8	2.0	3.4
B	56.5	28.7	8.4	1.1	0.7	0.4	1.2	2.0	1.0
C	55.0	30.5	1.5	1.1	0.3	0.1	6.6	2.8	2.2
D	74.8	13.4	1.3	0.6	2.7	0.6	3.4	1.1	1.9
E	83.3	10.0	0.2	0.2	0.8	0.0	1.9	2.2	1.4

Table 6. Concentrations of network modifiers $^{[5]}Fe^{2+}$ and $^{[5]}Fe^{3+}$ (molar mass) in glassy phases of the five fly ashes and the calculated index. Units have been normalised.

Fly ash	$^{[5]}Fe^{2+}$	$^{[5]}Fe^{3+}$	c_{NM}	n_{NF}	I	Compressive strength 28-day (MPa)
A	0.022	0.047	0.492	0.977	1.29	52.8 ± 1.6
B	0.006	0.002	0.294	1.196	0.70	43.7 ± 0.7
C	0.010	0.004	0.266	1.129	0.31	35.1 ± 1.5
D	0.006	0.009	0.177	1.182	0.18	16.5 ± 1.0
E	0.002	0.000	0.063	1.005	0.05	12.8 ± 1.2

Postprint of a paper published in *Cement and Concrete Research*, 85(2016):163-173. Version of record is available at http://dx.doi.org/10.1016/j.cemconres.2016.04.007

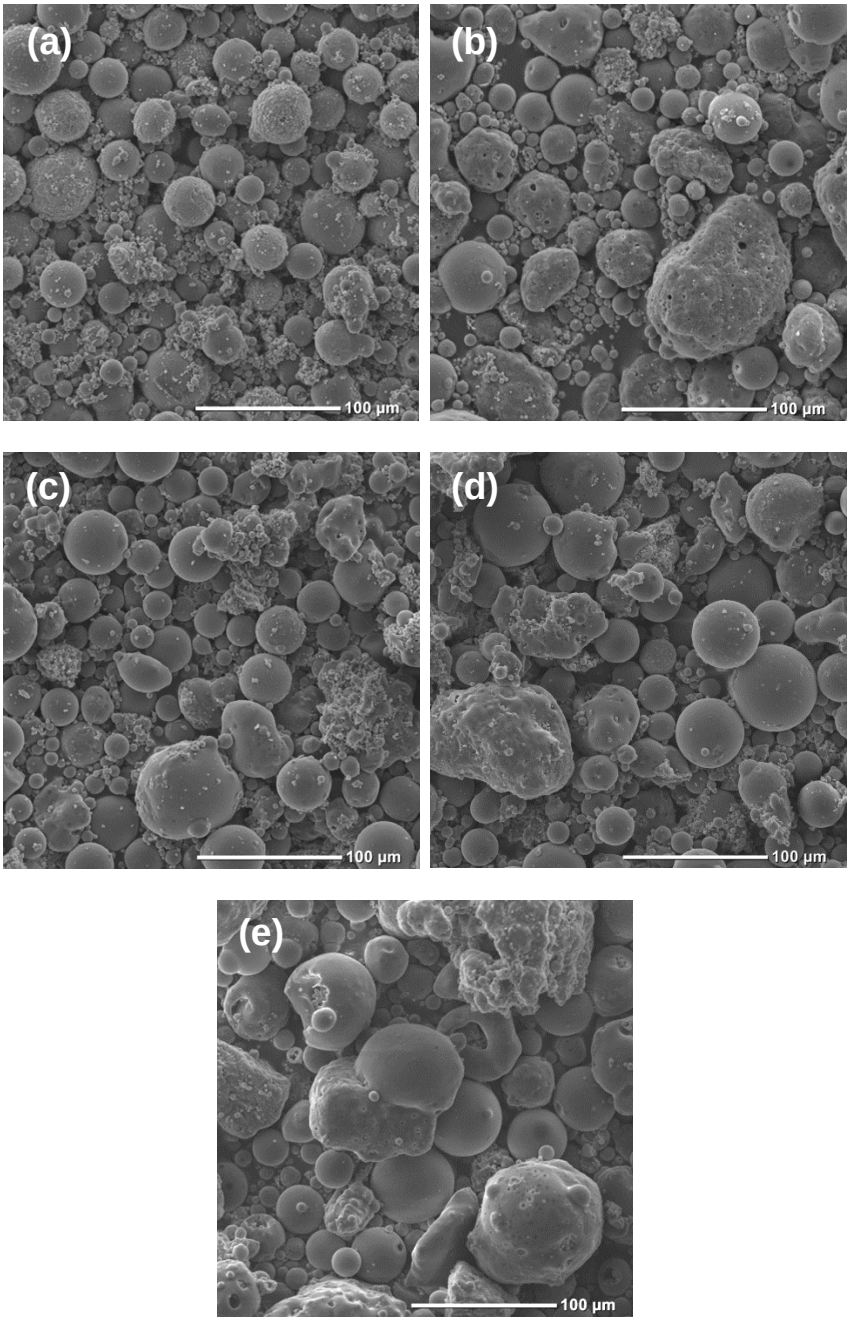

Fig. 1. SEM images of fly ash particles: a - e represent fly ashes A – E respectively.

Postprint of a paper published in *Cement and Concrete Research*, 85(2016):163-173. Version of record is available at http://dx.doi.org/10.1016/j.cemconres.2016.04.007

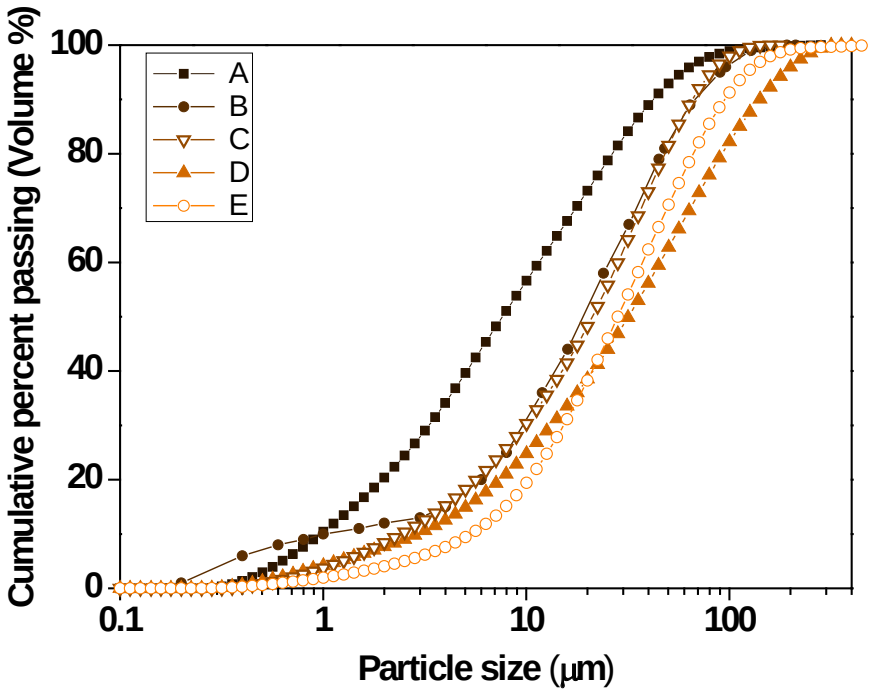

Fig. 2. Particle size distributions of fly ashes as determined by laser PSA.

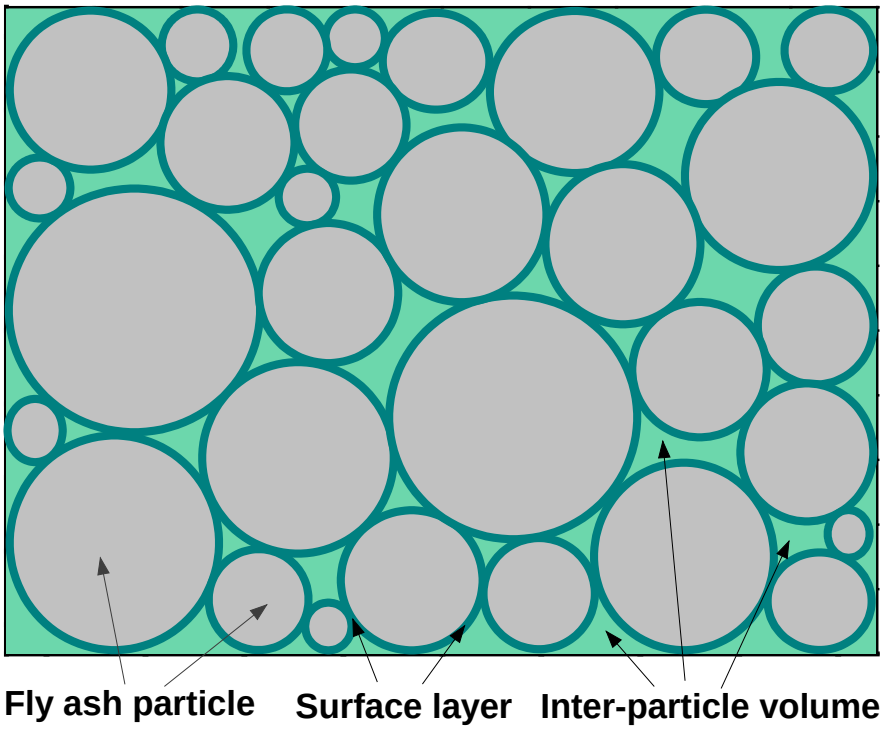

Fig. 3. A sketch of fly ash particles mixed with liquid activating solution showing the surface layer and interparticle volumes.

Postprint of a paper published in *Cement and Concrete Research*, 85(2016):163-173. Version of record is available at http://dx.doi.org/10.1016/j.cemconres.2016.04.007

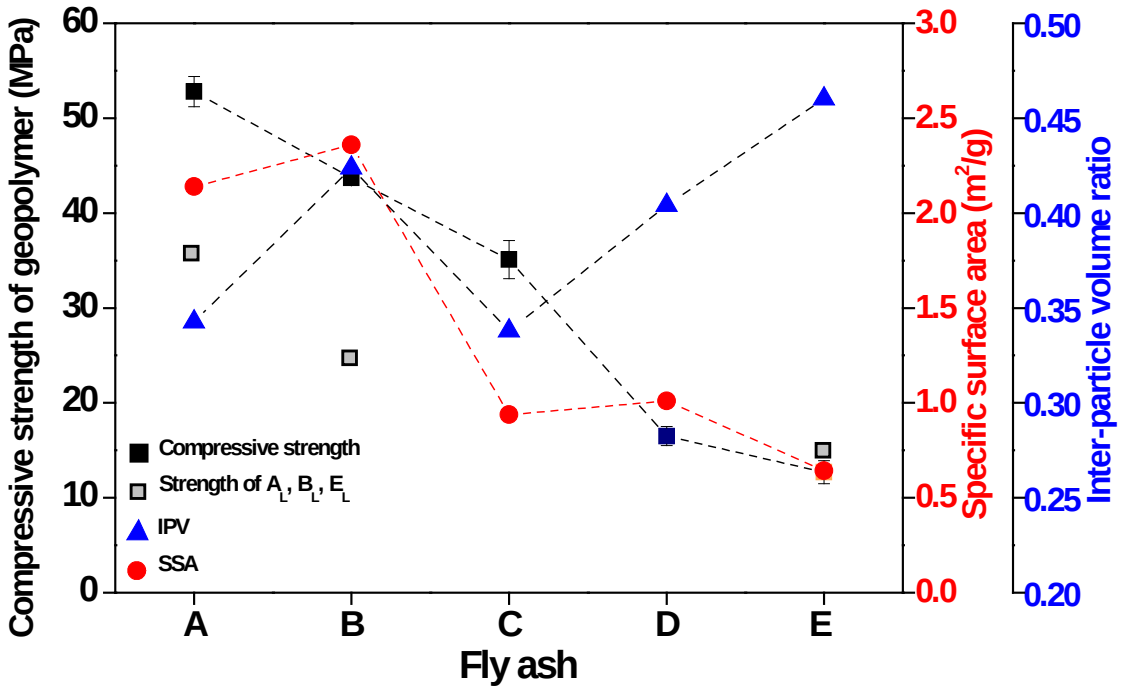

Fig. 4. The relationship between fly ash specific surface area (SSA), interparticle volume ratio (IPV) and compressive strengths of geopolymers obtained from each of the ashes studied. Lines are drawn as a guide to the eye only. Where error bars are not shown on strength measurements, the standard deviations are smaller than the symbols on the plot.

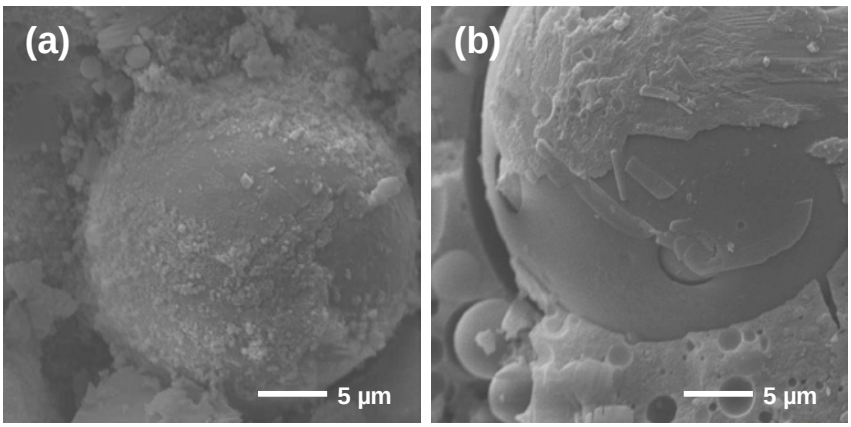

Postprint of a paper published in *Cement and Concrete Research*, 85(2016):163-173. Version of record is available at http://dx.doi.org/10.1016/j.cemconres.2016.04.007

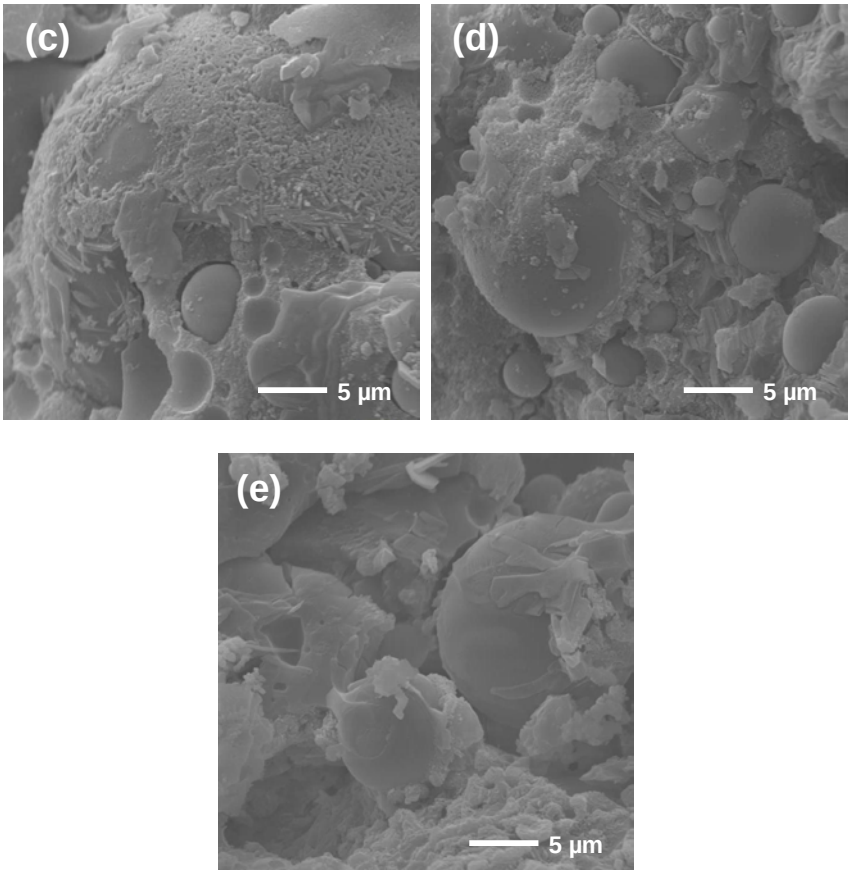

Fig. 5. SEM images of the cross sections of fractured geopolymers, showing the residual particles and the protruding crystalline phases after partial reaction: (a) to (e) geopolymers A to E respectively.

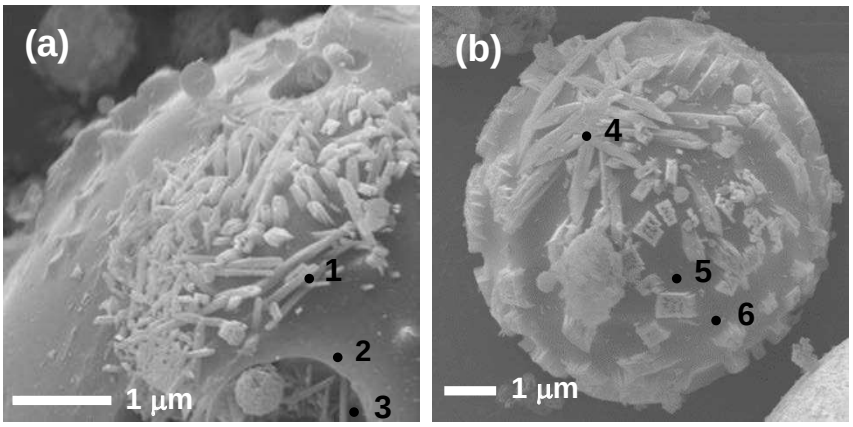

(d) Atom number percentages by EDS analysis, %. The remaining includes C and O atoms while Au has been excluded in calculation.

Postprint of a paper published in *Cement and Concrete Research*, 85(2016):163-173. Version of record is available at http://dx.doi.org/10.1016/j.cemconres.2016.04.007

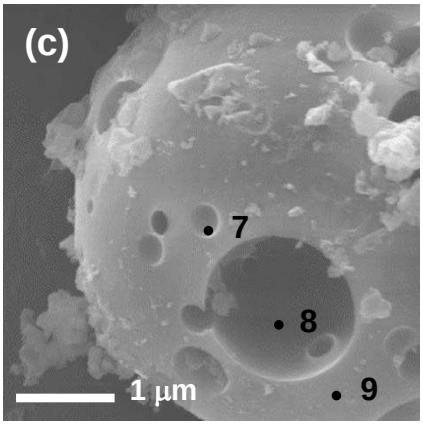

	Al	Si	K	Ca	Fe	Ti
1	13.8	11.7	-	-	-	-
2	7.7	12.9	-	1.7	1.3	-
3	11.3	14.2	-	2.3	1.4	-
4	14.9	13.6	-	-	-	-
5	9.3	16.4	0.6	-	0.3	-
6	9.6	17.3	0.7	-	0.2	-
7	10.0	30.1	0.2	-	-	-
8	6.3	17.3	-	-	-	0.1
9	3.6	20.7	-	-	-	0.2

Fig. 6. SEM-EDS analysis of NaOH-dissolved fly ash particles: (a) fly ash A; (b) fly ash B; (c) fly ash E and (d) compositions of the detected points in (a)-(c).

Postprint of a paper published in *Cement and Concrete Research*, 85(2016):163-173. Version of record is available at http://dx.doi.org/10.1016/j.cemconres.2016.04.007

Table 7. Re-examination of the fly ashes used in geopolymer synthesis and the relationship between reactivity index I and 28-day compressive strength (f_c)

Fly ash source	Particle density (g/cm^3)	SSA (m^2/g)	IPV	Glassy phase (%)	$^{[5]}Fe^{2+}$ (mol)	$^{[5]}Fe^{3+}$ (mol)	c_{NM} (mol)	n_{NF} (mol)	I	28-day f_c (MPa)	Notes
Collie (West Australian)	2.40	0.66	0.470	52.42	0.015	0.062	0.356	0.687	0.79	53 ± 10	Ref. [18]
Eraring (New South Wales)	2.02	0.46	0.434	60.7	0.006	0.007	0.185	0.920	0.21	33 ± 8	f_c was determined on the system with Si:Al = 2.5 and Na:Al = 1.25. The Na, Si and Al represent the available part from glassy phase and activator. Samples were cured at 70°C×24 h following by ambient temperature. Varying Si:Al and H:Si ratios in certain ranges show the same strength trend for the three fly ashes.
Tarong (Queensland)	2.00	0.50	0.431	49.77	0.001	0.005	0.041	0.796	0.06	26 ± 4	
Gladstone (Queensland)	2.20	1.00	0.471	76.87	0.013	0.032	0.378	1.152	0.70	19 ± 2	Ref. [20]
Amek (New South Wales)	2.00	0.50	0.416	67.50	0.005	0.012	0.325	1.007	0.39	7.5 ± 0.5	Density, SSA and IPV are calculated based on the composition and particle size information provided by the authors of [54]. The composition of geopolymers were designed to be constant at $Na_2O{\cdot}Al_2O_3{\cdot}3.8SiO_2{\cdot}13.6H_2O$ by considering glassy phase, activator and additional $Al(OH)_3$. Samples were cured at 45°C×24 h, followed by sealed storage.
Tarong (Queensland)	1.60	0.38	0.391	67.36	0.002	0.010	0.053	1.113	0.05	4.5 ± 1	
FA1 (South Korea)	2.00	0.80	0.484	71.40	0.007	0.023	0.229	1.10	0.34	8.7 ± 2.2	Ref. [53]
FA2 (South Korea)	2.25	1.10	0.508	80.80	0.016	0	0.676	1.06	1.23	41.6 ± 12	Density, SSA and IPV are estimated based on the composition and the particle size distribution. The activator was 5 M NaOH and used at constant solution/solid ratio of 0.6. Samples were at 60°C and RH = 99%.